Contents lists available at ScienceDirect

Computers & Graphics

journal homepage: www.elsevier.com/locate/cag

Generalized Abeille Tiles: Topologically Interlocked Space-Filling Shapes Generated Based on Fabric Symmetries

Ergun Akleman[b], Vinayak R. Krishnamurthy[a,*], Chia-An Fu[c], Sai Ganesh Subramanian[a], Matthew Ebert[a], Matthew Eng[c], Courtney Starrett[c], Haard Panchal[c]

[a] *J. Mike Walker '66 Department of Mechanical Engineering, Texas A& M University, College Station, Texas, 77843*
[b] *Department of Visualization & Computer Science and Engineering, Texas A& M University, College Station, Texas, 77843*
[c] *Department of Visualization, Texas A& M University, College Station, Texas, 77843*

ARTICLE INFO

Article history:

Tessellation of Space, Space-Filling Shapes, 3D Tile Design, Abeille Vault, Topologically Interlocking Shapes

ABSTRACT

In this paper, we present a simple and intuitive approach for designing a new class of space-filling shapes that we call Generalized Abeille Tiles (GATs). GATs are generalizations of Abeille vaults, introduced by the French engineer and architect Joseph Abeille in late 1600s. Our approach is based on two principles. The first principle is the correspondence between structures proposed by Abeille and the symmetries exhibited by woven fabrics. We leverage this correspondence to develop a theoretical framework for GATs beginning with the theory of bi-axial 2-fold woven fabrics. The second principle is the use of Voronoi decomposition with higher dimensional Voronoi sites (curves and surfaces). By configuring these new Voronoi sites based on weave symmetries, we provide a method for constructing GATs. Subsequently, we conduct a comparative structural analysis of GATs as individual shapes as well as tiled assemblies for three different fabric patterns using plain and twill weave patterns. Our analysis reveals interesting relationship between the choice of fabric symmetries and the corresponding distribution of stresses under loads normal to the tiled assemblies.

1. Introduction

In this paper, we present a simple and intuitive approach for designing a new class of space-filling shapes that we call Generalized Abeille Tiles (GATs). Space-filling shapes have applications in a wide range of areas from chemistry and biology to engineering and architecture [1]. Using space filling shapes, we can compose and decompose complicated shelled and volumetric structures for design and construction. Furthermore, if a given shape can be uniformly repeated to fill space, it is easier to mass produce using faster methods such as casting and injection molding instead of machining and additive manufacturing.

To date, most widely known space filling shapes are essentially regular prisms (e.g. rectangular bricks) since they are relatively easy to manufacture and are widely available. Reliance on regular prisms, on the other hand, significantly constrains our design space for obtaining reliable and robust structures [2, 3, 4, 5, 6]. While the interest in complex (and even non-convex) space-filling shapes has increased in the recent past [7], we find that the tool-box for systematically designing 2.5D and 3D space filling tiles is currently limited.

In this paper, we utilize this idea of fabric geometry to develop a framework for constructing a family of **topologically interlocking** space-filling shapes that can be designed with simple and intuitive *control*. According to Estrin et al. [8], *topological interlocking is a design principle by which elements (blocks) of special shape are arranged in such a way that the whole structure can be held together by a global peripheral constraint, while locally the elements are kept in place*

*Corresponding author: Email: vinayak@tamu.edu

by kinematic constrains imposed through the shape and mutual arrangement of the elements. The elements support each other by local kinematic constrains resulted from their shapes and mutual arrangements [9, 10, 11, 8]. Our general conceptual framework to design these shapes is based on partitioning the space using Voronoi decomposition by choosing high-dimensional Voronoi sites (curves and surfaces) and configuring these sites based on weave symmetries. This framework enables the design of a wide variety of topologically interlocking space-filling shapes that we call Generalized Abeille Tiles (GATs).

Fig. 1: (Photographs of Physical Fabrication of Shapes by 3D Voronoi Algorithm) Five views of an example of our generalized Abeille tiles, cast in aluminum. In this case, we used 3D Voronoi decomposition using Voronoi sites shown in Figure 10b

. Since the top and bottom are exactly the same planar shapes, these tiles can fill both 2.5D and 3D spaces.

1.1. Advantages

Our framework guarantees that the shapes (1) are space-filling (because of Voronoi-based approach) and (2) preserve the geometric characteristics of topologically interlocking blocks in any desired assembly (because of the symmetries of 2-way 2-fold woven structures). Symmetries of 2-fold fabric structures are useful since they provide a simple approach for designing symmetries. A particular subset of 2-fold fabrics, which is called 2-way, are particularly useful for simple and intuitive control. They include symmetries of the most popular weaving structures such as plain, twill and satin.

Using the properties of 2-fold 2-way fabrics, we have developed an interface to obtain desired symmetries. We have also developed a simplified method to compute Voronoi decomposition based on two principles. First, we only use fundamental domain of the particular symmetry. Second we sample high-dimensional Voronoi sites and compute 3D Voronoi decomposition for each sample point. This process gives us a set of convex Voronoi polyhedra for each Voronoi site. The union of these convex polyhedra gives us a desired GAT. Finally, we have also identified simple and robust algorithms to take union of all convex Voronoi polyhedra that comes from the same piece-wise linear curve segment. We demonstrate our approach through the design of several topologically interlocking space-filling tiles.

1.2. Our Contributions

Our overarching contribution in this work is a conceptual framework for generating space-filling and topologically interlocking tiles by utilizing spatial symmetries embodied by woven fabrics in conjunction with space decomposition using 3D Voronoi partition. Based on this framework, we make the following contributions:

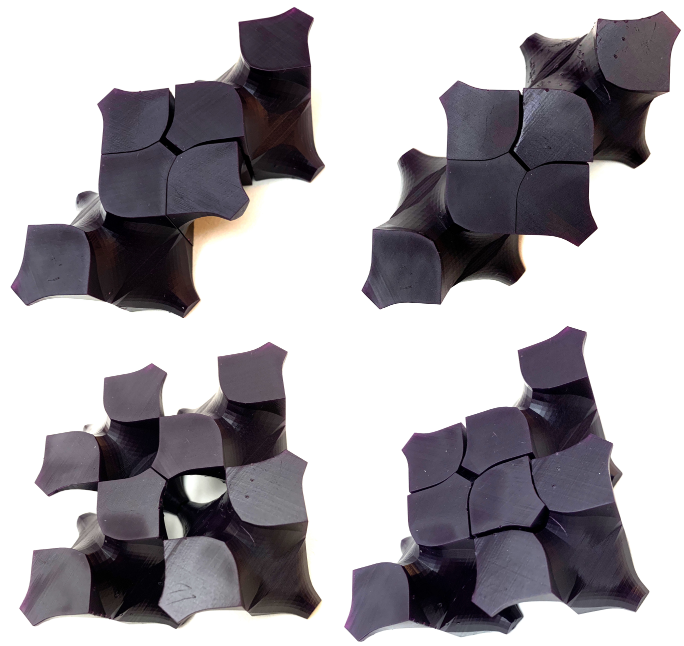

Fig. 2: (Photographs of Physical Fabrication of Shapes by 3D Voronoi Algorithm) Assembled wax models of a genus-0 space filling Generalized Abeille tiles demonstrating how they can fill 2.5D space.

1. We use our general framework to develop a simple and intuitive methodology for the design and construct *Generalized Abeille Tiles (GAT)*, space-filling tiles inspired by topologically interlocking assemblies. The basic idea is to use 1D trees and graphs in 3D assembled based on symmetries of 2-way 2-fold weaving patterns (such as plain and twill) as Voronoi sites for decomposing 3-space.

2. We have developed two methods to obtain GATs. The first method uses layer-by-layer Voronoi decomposition and Voronoi sites are ruled surfaces extruded along z axis such as the two triangles shown in Figure 9a and two concave hexagons shown Figure 10a (see section 3). The second method uses 3D Voronoi decomposition provided by 1-complexes, i.e. trees or graphs (see Figures 9b and 10b in section 3). The first method is very intuitive and it provides precise control over the results. In principle, we expected the 3D Voronoi decomposition to be computationally expensive and non-intuitive. However, we did not see any significant disadvantage in either computational efficiency or shape control. We further observed that the Voronoi sites themselves provide sufficient intuition on the final shapes.

3. Since we are only interested in single space-filling Abeille tile, we only need to solve problem in a domain that is large enough to obtain single tile. We, therefore, only decompose a prism that is slightly larger than fundamental domain of underlying symmetry (see Figure 19 in subsection 3.2).

4. Our algorithm for generating GAT is based on a simple yet novel approach that samples points from the Voronoi sites (such as trees, graphs, and ruled surfaces). Therefore, the Voronoi sites only act as guiding shapes rather than actual input to the Voronoi decomposition. Our algorithm first populates the guide shapes using a set of points and then constructs a Voronoi region that corresponds to Voronoi site simply by computing the union of *constitutive* Voronoi cells for each sample point. Figure 15 shows the method in one 2D layer. The first advantage of this method is its simplicity; it allows us to directly use standard Voronoi cell computation for any object. Secondly, it allows for an elegant computation of the surfaces of the Voronoi region as a triangle mesh using a simple topological operation; removing the internal polygonal faces of adjacent constitutive cells of points.

5. We also demonstrate that by controlling how to populate the original guide shapes we can control the shapes of the final structures (see Figure 11 in Section 3.2). The idea is also visible in comparing Figures 15a and 15b in Section 3.1. By changing the sampling density and sample locations from the same guide shape, we can obtain completely different tile geometries (e.g. two disconnected polygons or single polygon). This property allows us to control topology of the decomposition of space in each layer (see Figure 11 in in Section 3.1).

6. We present a comparative structural evaluation of three specific cases of GATs generated by plain- and twill-woven fabric symmetries. The finite element analyses (FEA) of the unit tiles and their assemblies under different loading conditions reveal that weaving allows distribution of planar and normal loads across tiles through the contact surfaces, generated with our methodology. We describe the qualitative relationship between the symmetries induced by the weave patterns to the stress distribution in the tiled assemblies.

2. Related Work

2.1. Topologically Interlocking Shapes

The inspiration for this paper came from Joseph Abeille's 1699 patent for flat tiles that are now known as Abeille vaults [12] (See Figures 4b and 3a). Abeille vaults are stones, generated by truncating two opposite edges of a tetrahedron, that can be assembled in a two-directional pattern resembling a woven fabric (Figure 4) to form self-supporting structures [13, 14]. Since then, several variants of these structures have been invented and studied under the name of topological interlocking assemblies (TIA) [9, 10, 11, 8]. These assemblies typically consist of a single unit element that can be repeatedly arranged in such a way that the assembled structure composed of this element can be held together by boundary constraints. Furthermore, each element itself is kept in place by local kinematic constrains imposed through the shape and mutual arrangement of the elements [9].

Medieval building masters have employed assemblies similar to Abeille's vaults. Early examples of similar assemblies, which are usually referred as stereotomy, can be found in Villard de Honnecout's fylfot grillage assemblies, Leonardo da Vinci's spatial structures, Sebastiano Serlio's planar floors, and John Wallis's scholarly work [15]. In these constructions a discrete load-bearing element supports two neighboring components, and is mutually supported by two others to span distances longer than their length [16, 17]. Abeille's vault was patented at the end of the 17th century as a class planar assemblies that could overcome the structural instability under the application of loads that are perpendicular to planar surface [18]. Other related terms topological interlocking are stereotomy [19, 13] and reciprocal frames or nexorades [20], which are used to refer ancient Asian forms of timber construction [21].

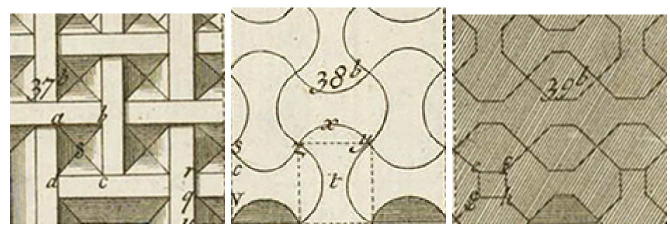

(a) Top View of flat Abeille vault. (b) Top View of Abeille vault with circular edges. (c) Top View of a Truchet vault.

Fig. 3: (Hand-Drawn Illustrations) 1738 Drawings of top views of Abeille and Truchet vaults by Frezier [22].

Sébastien Truchet discovered and patented another topologically interlocked module as a variant of Abeille's vault again using identical blocks in early 18th century [23, 24]. One of the advantages of both Abeille's and Truchet's patents is their ability to sustain loads and control the displacement of the blocks [25]. Both of these structural systems are capable of tolerating orthogonal and transverse forces [26]. However, for these assemblies to work the whole assembly process must be completed. Moreover, these assemblies require strong boundary support provided by structures such as buttresses or hefty walls [25]. Therefore, Abeille's shapes and their derived versions never really gained much popularity [27, 17] and were primarily used to build only a few flat vaults in Spain during late 18th and early 19th century [28]. It is only in recent literature that Abeille's creations received a renewed attention mainly in material design and architecture communities [29, 24]. Even then, most current research has only focused on either analyzing existing building blocks already proposed by Abeille and Truchet or creating curved structures from originally known blocks [23, 24]. As a result, even the physical evaluation of such structures remains limited to the original Abeille blocks.

We observe that the true potential of Abeille's work has not been completely realized in the context of geometric modeling and design of complex structures. This is because there seems to be no systematic way to discover similar building blocks. Moreover, most of these structures are not space-filling. There is, therefore, a need for formal approaches that enable intuitive design and *control* of a wide variety of modular and tileable building blocks. Our motivation is to cater to this need by developing and investigating a methodology to expose the vast design space of topological interlocked space-filling shapes.

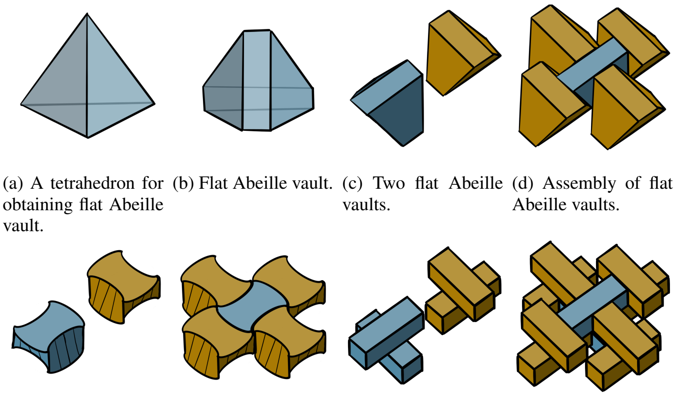

(a) A tetrahedron for obtaining flat Abeille vault. (b) Flat Abeille vault. (c) Two flat Abeille vaults. (d) Assembly of flat Abeille vaults.

(e) Two Abeille vaults with circular edges. (f) Space filling assembly of 4e. (g) Two Abeille type discrete elements. (h) Assembly of 4g.

Fig. 4: (Hand-Drawn Illustrations) Abeille tiles are mirror symmetric structures obtained by placing two identical shapes placed on top of each other with a relative rotation of 90^0. Each elemental shape is generated by truncating two opposite edges of a tetrahedron. Notice that yellow and blue tiles have identical shapes. We added 4h to visually demonstrate that these assemblies can be achieved using symmetry operations of plain woven fabrics as shown in 4g.

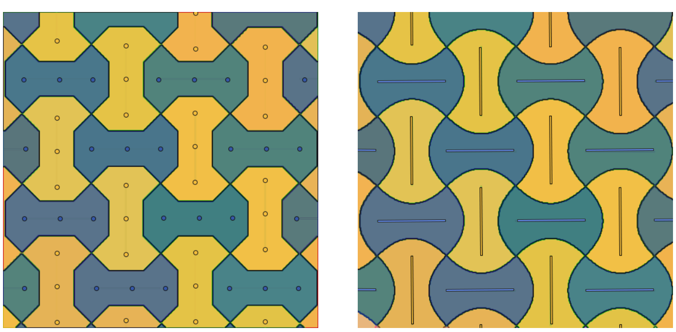

(a) Voronoi decomposition of 2D space using union of three points closed under symmetry of plain woven fabrics. (b) Voronoi decomposition of 2D space using line segments that are closed under symmetry of plain woven fabrics.

Fig. 5: (Computer Generated Illustrations) We can obtain shapes that are visually similar top views of Abeille type tiles using Voronoi decomposition of domains that are closed under symmetry of plain woven fabrics. Notice that in (5b), the curved segments are paraboloid (non-circular) arcs, but overall shapes still appears the same.

2.2. *Voronoi Decomposition*

Our framework is based on the observation that we can obtain shapes similar to Abeille and Truchet vaults by decomposing the 3D space with Voronoi diagrams using Voronoi sites that are closed under symmetries of plain woven fabrics. These Voronoi sites, of course, need to be higher dimensional such as lines, curves, trees or graphs. Union of a set of points is also useful. Figure 5a shows that Voronoi decomposition using a wallpaper pattern of union of three points can produce top-view of Flat Abeille and Truchet tiles. Figure 5b further demonstrate that the shapes that resemble the top view of Abeille vaults with curved edges (See Figure 3b) can be obtained with lines that are closed under symmetries of plain woven fabrics. We note that this observation is also in sync with Delaunay's original intention for the use of Delaunay diagrams. He used symmetry operations on points and Voronoi diagrams to produce space filling polyhedra, which he called Stereohedra [30, 31].

2.3. *Abeille's Vault & Fabrics*

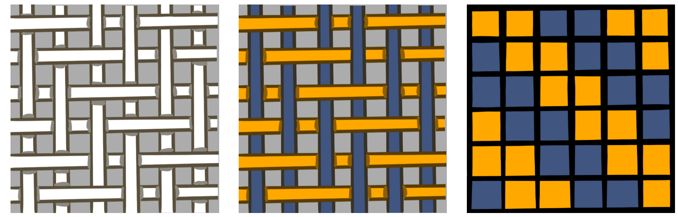

(a) *Top view of* $(2, 2, 1)$ *twill weave with uncolored threads.* (b) *Same weave with colored warp and weft threads.* (c) *Matrix view of the* $(2, 2, 1)$ *twill weave.*

Fig. 6: (Hand-Drawn Illustrations) The fundamental domain of 2-way 2-fold fabrics is a rectangle and they can be represented as a simple matrix. The warp threads are colored blue and weft threads are colored yellow to differentiate the two threads in the final matrix. Symmetries can be obtained by the matrix.

This paper also grew out of the visual analogy between symmetries of plain woven fabrics and assembly of truncated tetrahedra (and their variants) that are used in topological interlocking (See Figure 4). This visual analogy, which is also observed by others such as Borhani and Kalantar [13], indicates that many (and perhaps all) other fabric geometries can be used to develop methods to design topologically interlocking shapes.

The first observation we make in this work is regarding the relationship between Abeille's original structural construction and weaving patterns in fabrics. A 2D projection of the classic vault from Abeille shows a remarkable resemblance to the projection of the classic plain-weave pattern that is commonplace in fabrics. Therefore, we posit that the geometry and topology of fabric structures provides an elegant and intuitive method for generalizing the notion of Abeille's vaults. Based on this, our approach is to leverage 2D projections of fabric patterns as the starting point for generating generalized Abeille tiles.

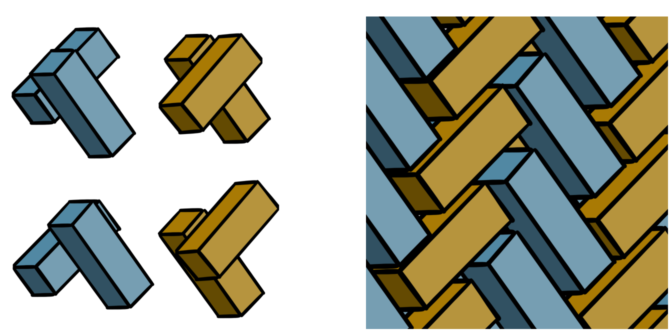

(a) ((2, 2, 1) Twill Abeille type elements. All elements are the same. (b) Assembly of these Abeille elements appears to be a twill woven fabric.

Fig. 7: (Hand-Drawn Illustrations) The other Abeille type tiles (the blue and yellow two-element combinations in sub-figure (a)) are mirror symmetric shapes obtained by placing two same shapes top of each other with 90^0 rotation. The only difference is the pivot point of rotation. They are assembled using symmetry operations of other 1-fold 2-way woven fabrics such as twill.

2.4. *Woven Fabrics*

Most common woven fabrics are *biaxial*, or 2-way and 2-fold, which consist of two strands, i.e. 2-way that are called warp and weft. The word 2-fold originated from the behavior of the weft strands that pass over and under warp strands,

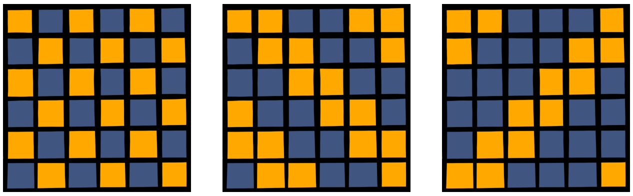

Plain: $[1, 1, 1]$ Twill: $[2, 2, 1]$ Twill: $[2, 3, -1]$

Fig. 8: (Hand-Drawn Illustrations) Matrix view of plain and twill patterns.

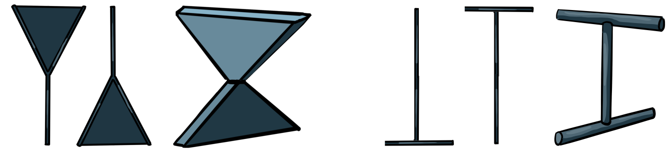

(a) Two mirrored and 90^0 rotated triangles.

(b) Two mirrored and 90^0 rotated T shapes.

Fig. 9: (Hand-Drawn Illustrations) Front, side and 3D perspective view of the basic Voronoi sites we have initially used to obtain space filling Abeille tiles.

which corresponds to thickness of the fabric. The mathematics behind such 2-way, 2-fold woven fabrics such as plain, satin and twill, were first formally investigated by Grunbaum and Shephard [32]. They also coined the word, isonemal fabrics to describe fabrics that have a transitive symmetry group on the strands of the fabric [33] (See Figures 6 and 8). Chen et al. showed that it is useful to express the woven pattern by two integers a and b, where a is the number of up-crossings, and b is the number of down-crossings where $a + b = n$ and an additional integer s still denotes the shift introduced in adjacent rows [34]. Any such weaving pattern can be expressed by a triple $[a, b, s]$. The Figure 8 also shows a basic block of a biaxial weaving structure and the role of these three integers, $a > 0$, $b > 0$ and $0 < s < a + b$ [1]. Figure 8 shows plain and twill weaving structures that can be described by the $[a, b, s]$ notation. Using this notation, it is possible to name and construct each weaving structure uniquely. Figures 4 and 7 show how to create corresponding assemblies.

3. Methodology

The inspiration for our computational methodology to construct GATs came from a recent work on Delaunay Lofts [7] and other earlier works [35, 36]. In that work, curves along z axis are used to construct space-filling structures that resemble scutoids[37, 38]. We observe that in case of Delaunay lofts, it is possible to control shapes of polygons in each layer by directly controlling symmetry structures. However, a single curve does not work for Abeille tiles since we also need to control orientation of the polygons in each layer. Moreover, we may even have connected and disconnected polygons. We observed that we can obtain desired control by using two curves that defines a ruled surface. The section 3.1 provides the method in detail. We later realized that we do not really need a layer-by-layer approach to have control and we have developed a method that uses 3D Voronoi decomposition. The section 3.2 provides that method in detail.

Based on this basic idea, we designed several specific types of tiles by choosing Voronoi sites from basic property of Abeille tiles: two mirrored and 90^0 rotated shapes that are placed top of each other as shown in Figure 4g. These Voronoi sites can simply be a shape that connects two perpendicular lines as shown in Figure 9. The Voronoi site shown in Figure 9a consists of two triangles that can be converted into a GAT by using layer-by-layer 2D Voronoi decomposition (see section 3.1). When we use 3D Voronoi decomposition, it is possible to simplify Voronoi sites into a T-shaped configuration as shown in Figure 9b. Section 3.2 discuss 3D Voronoi decomposition to create the GATs. These basic structures are assembled using symmetry operations of two-way two-fold woven structures.

[1]The value of s can be any integer, however, $[a, b, s]$ and $[a, b, s + k(a + b)]$ are equivalent since $s + k(a + b)) \equiv s \mod (a + b)$. Therefore, we assume that the value of the s is between 0 and $a + b$.

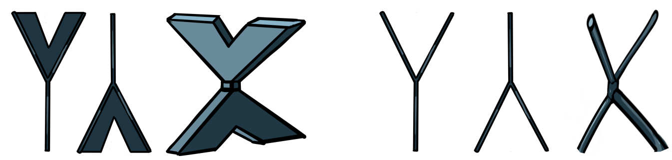

(a) Two mirrored and 90^0 rotated concave hexagons.

(b) Two mirrored and 90^0 rotated V shapes.

Fig. 10: (Hand-Drawn Illustrations) Front, side and 3D perspective view of V shaped Voronoi sites we have used.

Figure 10b provides one of the most effective Voronoi site examples we used. We eventually decided that two-V (or its variants two-U and two-Y) shapes are the most effective since they can provide additional interlocking capability (Figure 10). The Voronoi site shown in Figure 10a consists of two "*concave hexagons*" that can also be converted into a GAT by using layer-by-layer 2D Voronoi decomposition (see section 3.1). When we use 3D Voronoi decomposition, it is again possible to simplify the Voronoi sites into a V-shaped configurations (Figure 10b, see Section 3.2 for details). These basic shapes are also assembled using symmetry operations of 2-way 2-fold weaves.

Figures 1 and 2 shows physical (3D-printed and molded) Generalized Abeille tiles that are obtained by using Voronoi sites shown in Figure 10b that is assembled with plain woven symmetry. These particular shapes can interlock better (Figure 2) as dictated by plain weaving. We then experimented with a wide variety of Voronoi sites that exhibit the basic property of Abeille tiles.

3.1. Layer-wise Generation Algorithm

Our layer-wise algorithm extends Delaunay lofts [7]. Here we use ruled surfaces that is defined by two curves to obtain layer by layer Voronoi decomposition. Without loss of generality, we will explain the method by creating z constant layers in the domain of $0 \leq z \leq 1$. Our algorithm consists of seven steps as follows.

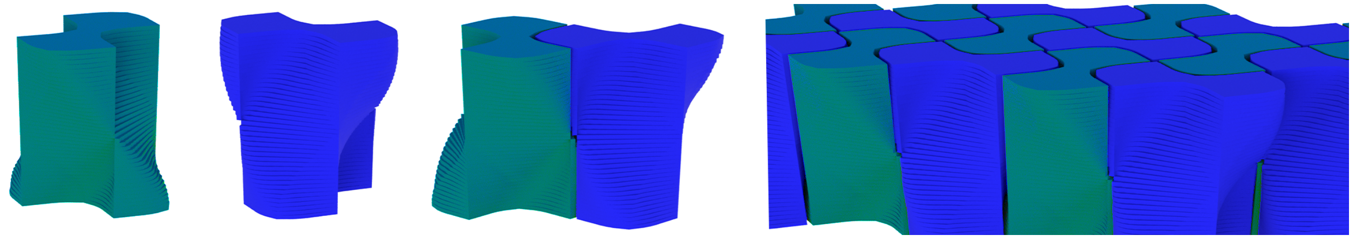

(a) Centers of the lines are sampled. The two single tiles blue and green tiles have identical mirror-symmetric shapes. It also shows two-tile and multi-tile assemblies.

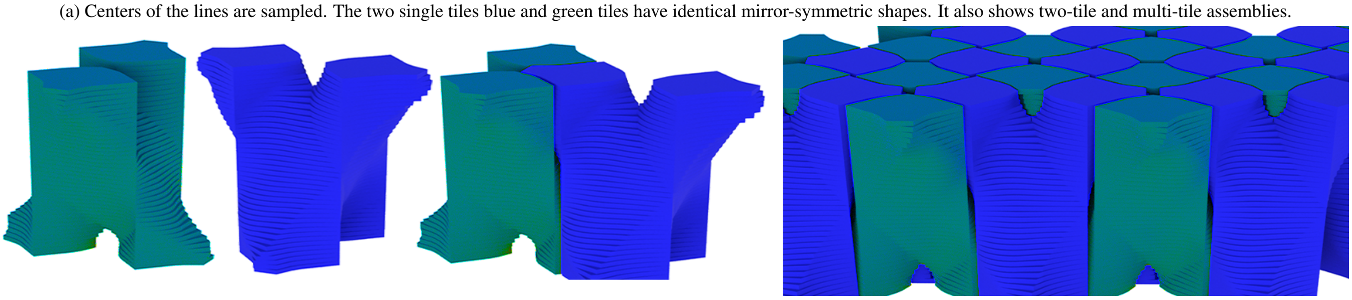

(b) Centers of the lines are not sampled. The two single tiles blue and green tiles have identical mirror-symmetric shapes. It also shows two-tile and multi-tile assemblies.

Fig. 11: (Renderings of Virtual Shapes by Layer-wise Generation Algorithm Output) Effect of sampling in plain woven Abeille tile design. By making line longer and not sampling center portion, we created additional interlocking.

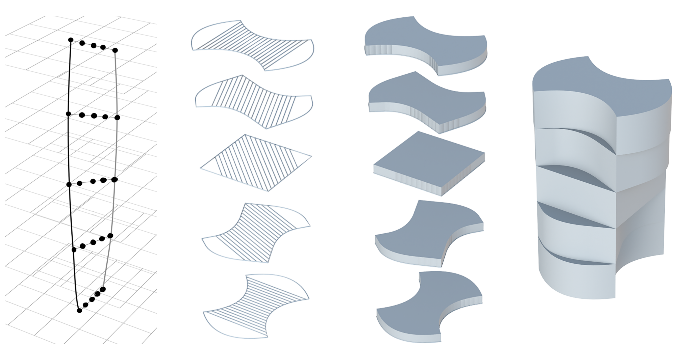

(a) The original Ruled Surface with five layers. (b) Five polygons in each of the five layer. (c) Five extruded polygons. (d) Union of five extruded polygons.

Fig. 12: (Renderings of Layer-wise Generation Algorithm Steps) The basic steps of our algorithm that provides layer by layer Voronoi decomposition for a given ruled surface.

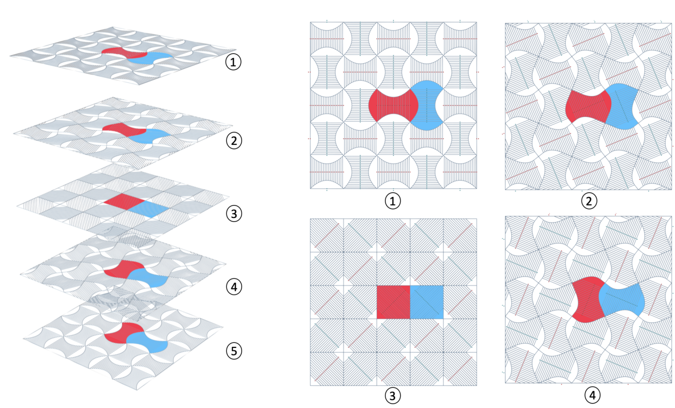

Fig. 13: (Renderings of Layer-wise Generation Algorithm Steps) Voronoi Decomposition obtained by using samples. Red and blue regions are obtained by taking union of Voronoi regions that comes from the same lines.

1. Define a ruled surface (see Figure 12a for an example) as:

$$
\begin{aligned}
F_x(z,t) &= x_0(z)\,(1-t) + x_1(z)\,t \\
F_y(z,t) &= y_0(z)\,(1-t) + y_1(z)\,t
\end{aligned}
$$

2. Populate the space with this ruled surface by using one of the symmetries of 2-way 2-fold fabrics. This process gives us a set of ruled surfaces $j = 0, 1, \ldots$ as follows:

$$
\begin{aligned}
F_{j,x}(z,t) &= x_{j,0}(z)\,(1-t) + x_{j,1}(z)\,t \\
F_{j,y}(z,t) &= y_{j,0}(z)\,(1-t) + y_{j,1}(z)\,t
\end{aligned}
$$

   In a given rectangular prism domain, which is chosen to be larger than fundamental domain of the symmetry (Figure 13).

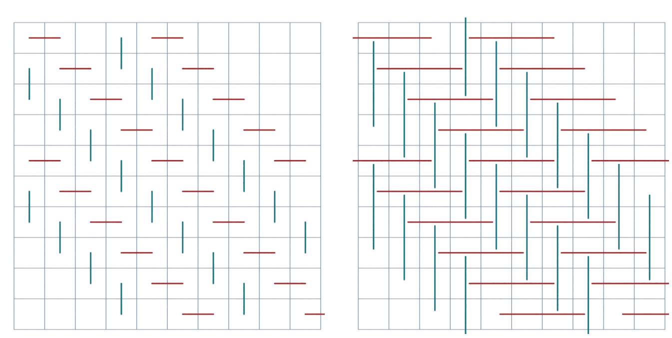

(a) Top layer for twill case in Figure 16a. (b) Top layer for twill case in Figure 16b.

Fig. 14: (Renderings of Layer-wise Generation Algorithm Steps) These examples shows the control lines that are used to construct twill Abeille tiles shown in Figure 16.

3. Define $n+1$ number of layers as $z = i/n$ planes where $i = 0, 1, \ldots, n$. The Figure 12 shows an example with five layers. Find intersection of the Voronoi site with each layer.

Since the Voronoi site is a ruled surface extruded along z direction, all intersections are lines that are given by their two endpoints

$$
\begin{aligned}
F_{i,j,x}(t) &= x_{j,0}(i/n)\,(1-t) + x_{j,1}(i/n)\,t \\
F_{i,j,y}(t) &= y_{j,0}(i/n)\,(1-t) + y_{j,1}(i/n)\,t
\end{aligned}
$$

4. Sample each line and compute Voronoi decomposition in each layer (see Figure 13).
5. Take the union of all Voronoi polygons that belong the same line. This operation gives us polygons shown in 12b. They are shown as red and blue polygons in Figure 13.
6. Extrude each polygon in z to obtain a set of polyhedra (see Figure 12b).
7. Finally, take the Union of the Extruded Polygons. The extrusion depth amount must be set equal to the distance between each layer such that each polyhedra to touch and rest on other layers.

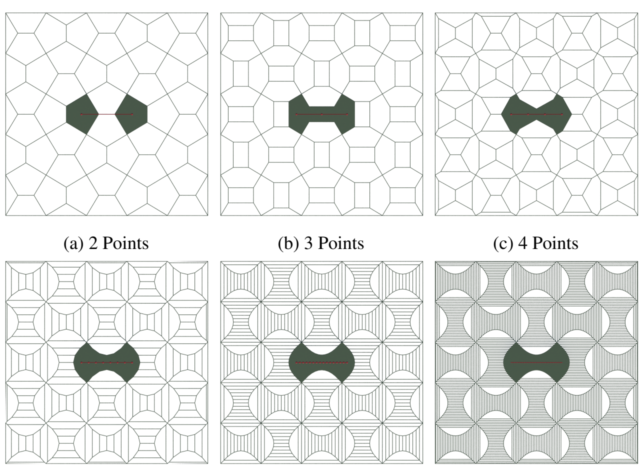

(a) 2 Points (b) 3 Points (c) 4 Points

(d) 8 Points (e) 16 Points (f) 32 Points

Fig. 15: (Layer-wise Generation Algorithm Output) Adjusting the point density on the Voronoi Site Guide Lines.

3.2. 3D Generation Algorithm

To evaluate the efficiency of layer-wise Voronoi decomposition, we decided to produce generalized Abeille tiles using 3D Voronoi decomposition. We determined that 3D Voronoi decomposition is also simple and intuitive. In our first attempt, even by using very low number of sample points, we obtained promising results (Figure 17). We can also control results by changing number of positions of sample points (Figure 18). Another advantage of the 3D Voronoi is that the algorithm is extremely simple. We only need to take union of convex polyhedra resulted from 3D Voronoi decomposition of 3D points. We also need to consider only a fundamental domain (Figure 19).

Taking union of all Voronoi regions belonging to the same guide shape (Voronoi site) to obtain desired space filling tile can be implemented a set of face removal operations. Specifically, the shared faces of two consecutive convex polyhedra coming from two consecutive sample points on the curve are deleted. Note that these faces will always have the same vertex positions with opposing order. If underlying mesh data structure provides consistent information, this operation is guaranteed to provide a 2-manifold mesh. Even if the underlying data structure does not provide consistent information, the operation creates a disconnected set of polygons that can still be fabricated through additive manufacturing.

4. Structural Evaluation

The mechanics and geometry of Abeille-type structures are closely connected as shown earlier by Brocato et al. [27, 17, 21]. These mechanical investigations are primarily focused on the interaction between the faces in contact between two adjacent pieces — what Brocato et al. refer to as Abeille-bond. Therefore, the overarching topology of the structure/assembly composed of the Abeille-shaped "*bricks*" has a major effect on the mechanical behavior of the structure. Our aim was to observe how different weave symmetries induce different mechanical behavior compared to the flat Abeille vault. For this, we conducted several simulations of GAT assemblies using finite element analysis (FEA) and compared them with Abeille's original flat vault as well as a solid object as our benchmark.

4.1. Evaluation Rationale

Consider a solid continuous rectangular block of some finite thickness fixed to an inertial frame on the boundaries. Now, let us suppose that the center of this block is displaced by some load along the thickness of the block. In the context of topological interlocking, the stress distribution induced by such a displacement on this block represents our absolute benchmark. Therefore, in our evaluation, we seek to investigate the interlocking properties of GAT assemblies by comparing the magnitude and concentration of stresses induced by a displacement of one tiles (say the central tile without the loss of generality). We further note that high stress regions will occur at the interacting surfaces between two neighboring tiles. With this in view, we make three main observations: (1) higher magnitude of interface stress will imply better inter-locking; (2) the regularity of distribution and concentration of stress will imply better stability against perturbations in loading conditions.

Block Equivalent. In order to compare with our benchmark scenario, our first step was to conduct FEA simulations on a solid block of dimensions identical to the assemblies (box equivalent). The mechanical properties of this box equivalent would serve as a reference for us to compare the degree of tightness of inter-connectivity in between the unit GATs.

Flat Abeille vault. We further wanted to evaluate Abeille's original vault design. Abeille's original flat tiles are parametric structures which can be arranged together to form an assembly (Figure 4d). This assembly, though not space filling, can be held together simply by fixing the tiles in the perimeter. Khandelwal et al. [40] showed that the force–displacement response for topologically interlocked structures, specifically based on

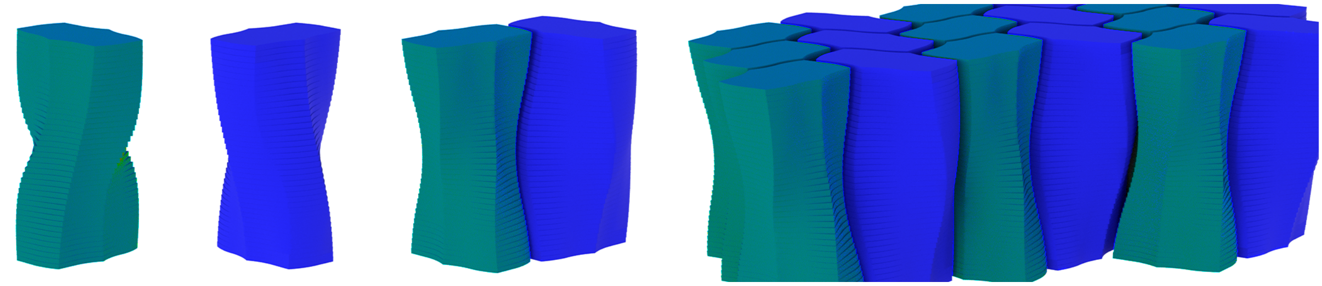

(a) Twill Abeille tile obtained using short lines shown in Figure 14a. The blue and green tiles have identical mirror-symmetric shapes.

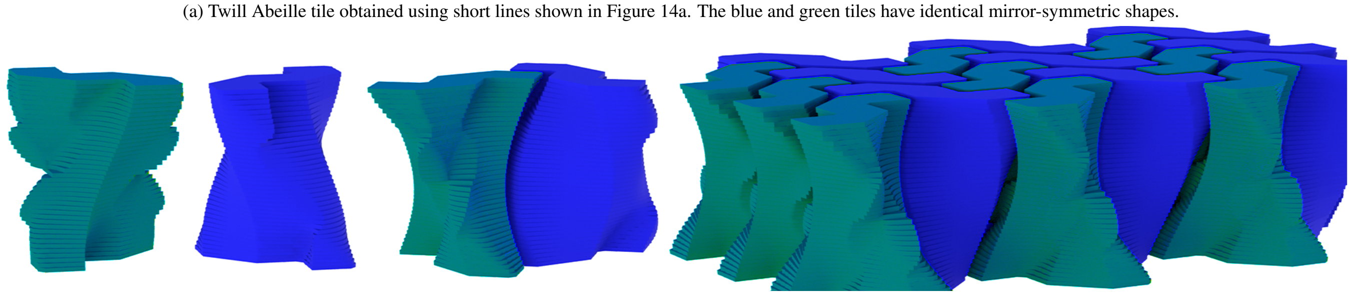

(b) Twill Abeille tile obtained using long lines shown in Figure 14b. The blue and green tiles have identical mirror-symmetric shapes.

Fig. 16: (Renderings obtained by Layer-wise Generation Algorithm Output) Examples of twill woven Abeille tile designs that demonstrate the effect of line lengths. These are obtained by layer-by-layer algorithm.

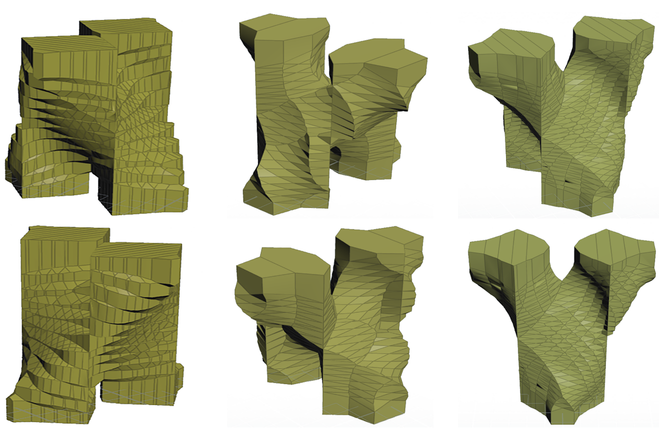

(a) Two-U skeleton. (b) Two-V skeleton. (c) Two-Y skeleton.

Fig. 17: (Renderings obtained by 3D Generation Algorithm) Examples from first 3D Voronoi attempts. We experimented with two-V, two-Y and two-U shaped Voronoi sites using low number of sample points.

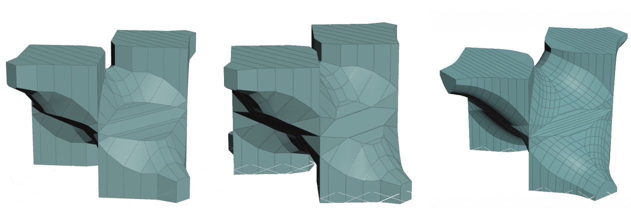

Fig. 18: (Renderings obtained by 3D Generation Algorithm) We also experimented with the number and positions of sample points in plain woven Abeille tile design using 3D Voronoi decomposition. Increasing the number of sample points helps to obtain smoother looking surface as expected.

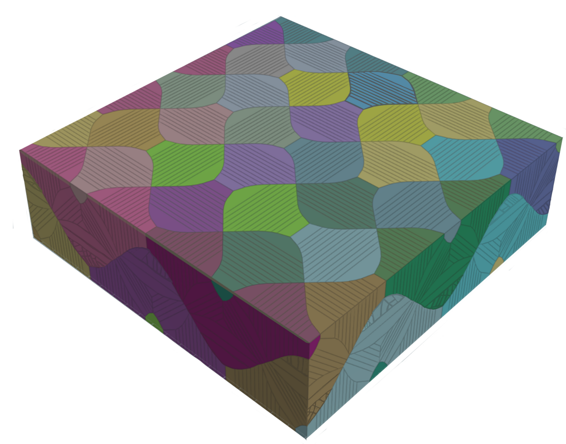

Fig. 19: (Rendering of fundamental domain) An example that shows a 3D Voronoi decomposition of fundamental domain (see [39] for the definition of fundamental domain). Note that the tiles in boundary is cut. This fundamental domain can be repeated in all three directions to fill the whole 3D space.

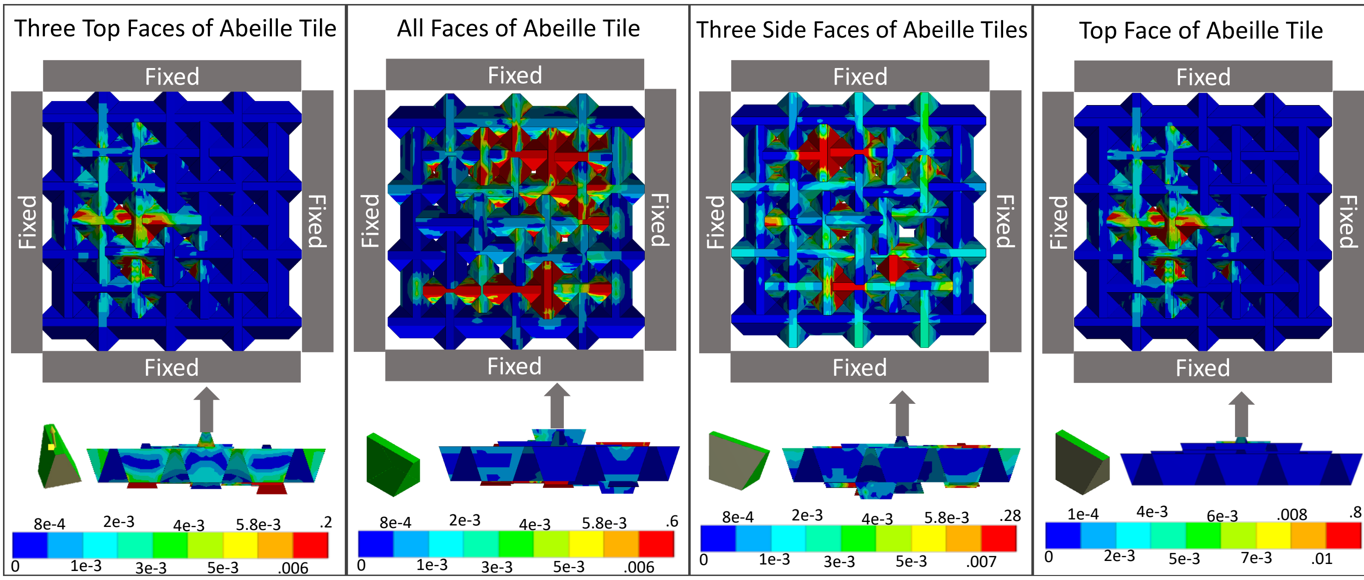

Fig. 20: (Simulation) This shows the stress distribution on a 7x7 assembly of Abeille tiles with different amounts of faces with forced displacement. In the first case the top face and the two larger side faces were forced with a displacement of 2mm. The third case shows when the top face and the two smaller side faces have a forced displacement. All stress values are in Pa. This means there is very little force needed to get a displacement of 2mm.

Abeille's flat vaults, exhibited an ideal softening response even though the individual blocks (tiles) were made out of brittle material. We study the mechanical response of these tiles separately and also compare it with the results we obtain for GATs.

Generalized Abeille Tiling. The shape of a unit GAT depends on two key factors. The first is the construction methodology (layer-wise 2D or 3D Voronoi decomposition). The second is the shape of the Voronoi sites. While the construction methodology results in minor differences between the shapes (in terms of continuity and smoothness of the contact surfaces), it is the configuration of the Voronoi sites that fundamentally affects the shape of each unit tile and consequently the interactions between those unit tiles in a given assembly of tiles. Furthermore, notice that the configuration of the Voronoi sites is based on the symmetries of the fabric weaving patterns. Therefore, in order to explore the relationship between the weave symmetries and the corresponding GATs, we considered two commonly known plain and twill weaves and analyzed their response to basic mechanical loading conditions. We specifically investigated the following cases:

1. **PA2D**: Plain-Abeille tiles generated using the layer-wise algorithm with T-shaped Voronoi sites (Figures 12d).

2. **TW2D**: Twill-Abeille tiles generated using the layer-wise algorithm with T-shaped Voronoi sites.

3. **PA3D**: Plain-Abeille tiles generated using the 3D Voronoi decomposition with V-shaped Voronoi sites (Figures 17c).

4.2. Evaluation Methodology

We assembled a 7×7 grid of the three GAT cases without any gaps between the parts. The contacts between the tiles are assumed to have zero friction. A displacement of 2mm was assumed to act vertically upwards out of the plane of the assembly. The border tiles in the assemblies were assigned as fixed supports. All possible contact regions between were made friction-less. This ensures that the stress induced in the assembly is solely due to the geometry of the tile itself. Mesh quality was set to default (0.5). The von-mises stress [41] and the total deformation color plots are then computed for each case (Figure 21). We conducted a static structural analysis for all simulations using the ANSYS Workbench 2019 R1.

Assumptions. The volume of each of the unit shapes are assumed (and modeled) to be equal. This, allows to make a fair comparison of the behaviour of these shapes when subjected to loading. Appropriate end faces were assumed as fixed support for every simulations and all the forces and moments were applied on the faces directly. All the simulations are done by assuming appropriate faces of central tile displaced by a constant distance of 2mm. All materials were assumed to be Polylactic acid (PLA) (density = 1250 kg/m^3, Young's modulus $E = 3.45 \times 10^3 MPa$, Poisson's Ratio $\nu = 0.39$).

4.3. Results and Observations

4.3.1. GATs vs Box equivalent

Since the block essentially represents a continuous connected version of the assembly it would offer the highest resistance to external disturbances. This can be be seen from the maximum value of average stress (20.35 Pa). We find that the average stress induced in the 3 cases **PA2D**, **TW2D**, and **PA3D** is of the same order of the Block equivalent.

The block has three regions of displacement: (1) constant region at the center, (2) a linearly decreasing region from the center to periphery, and (3) fixed periphery (Figure 21). Interestingly, the **TW2D** pattern exhibits similar displacement profile.

On the other hand, the **PA2D** and **PA3D** cases exhibit a decreasing continuity in the displacement profile. **PA3D** specifically shows a highly local displacement profile suggesting a higher interlocking ability again owing to the V-shaped Voronoi site. Finally, we note that the average displacement for the GAT assemblies are all lesser (albeit marginally) than the solid block. This, again, indicates good inter-locking ability.

4.3.2. GATs vs Flat Abeille Vault

The values of stress found in the flat Abeille vault, however, is orders of magnitude lesser than any of the generated tilings (Table 1). This clearly shows that the Abeille tiling doesn't offer high resistance to external disturbances. The implication is that GATs are tightly topologically interlocked when compared to flat Abeille vaults. The second crucial observation we made was that lack of symmetry in stress distributions for Abeille's flat vaults despite the fact that the assembly follows plain woven weave symmetry aking to some of our own assemblies. To investigate this further, we performed additional tests wherein we displaced different combinations of faces on the central element of the tiling. The resulting stress distributions still do not exhibit any observable symmetry or even consistency with respect to the other loading variations. This strongly indicates the lack of structural stability meaning that small perturbations in load can lead to large variations in how stresses are distributed to neighboring elements. We believe that the primary reason for this is the planar interface between two Abeille elements as opposed to curved convex-concave interfaces in GATs. This geometric property of GATs allows for a smoother propagation of contact stresses between neighboring elements resulting in a topologically consistent stress distribution.

4.3.3. Stress distribution patterns in GATs

Each of the three GAT cases exhibit distinct stress distribution patterns. Our goal is to compare these with the solid cuboidal block that exhibits a radially smooth variation of stress with concentration near the boundary which is fixed. In case of **PA2D**, we observe that the stress distribution is separated in two mutually perpendicular directions corresponding to the two axes of the bi-axial plain weaves. What is interesting is that the stresses on the top and bottom layers alternates between tiles aligned along the same direction, This is because a majority of stress transfer between two orthogonal tiles primarily takes place in the neck region of the tiles. For **TW2D**, we notice that the stress on the top and bottom layers is more uniformly distributed. However, this too alternates across orthogonal tiles. The stress distribution for **PA3D** is the most sparse distribution shaped as two rings induced on either side of the V-shape. We also observe an outer octagonal ring. This is likely due to the inter-tile interactions between the shapes induced by the V-shaped Voronoi sites. Unlike GATs, the flat Abeille vault does not have any distribution pattern or symmetry as previously noted.

4.3.4. Comparison across GATs

We observe a dissimilar behavior between **PA2D** and **PA3D** assemblies in terms of the maximum stresses (232.2 MPa and 153.02 MPa respectively). However, the average stresses are similar (7.78 MPa and 7.87 MPa) for these two cases when compared to **TW2D** (9.97 MPa). The most noticable observation is that the **TW2D** tiles experience the highest extremal stresses (7.28e-1 MPa and 404.82 MPa) in comparison to the other two cases. This is likely because of the high curvature neck regions in the **TW2D** tiles.

	Block	**PA2D**	**TW2D**	**PA3D**	Abeille
Stress (MPa)					
Min.	3.11e-11	1.15e-6	7.28e-1	9.45e-10	1.81e-14
Avg.	20.35	7.78	9.97	7.87	2.75e-9
Max.	94.18	232.2	404.82	153.02	2.86e-7
Displacement (m)					
Min.	0.00	0.00	0.00	0.00	0.00
Avg.	4.69e-4	3.46e-4	3.71e-4	3.15e-4	3.51e-4
Max.	2e-3	2e-3	2e-3	2e-3	2e-3

Table 1: Minimum, maximum and average stresses and displacements for tile assemblies when the center tile is subjected to a displacement of 2mm.

5. Discussion

5.1. Limitations

There are several limitations of our methodology. First, in the current work, we focus on only symmetries of 2-way 2-fold fabrics to simplify our explorations. Even simply considering the symmetries of 3-way 2-fold fabrics can significantly extend the design space [42]. Second, although the resulting tiles will still be space-filling (owing to Voronoi partitioning), the connections in z-direction are not really interesting: they are flat. For true 3D space filling tiles, the symmetries must go beyond 2.5D symmetries that are extended from 2D wall paper symmetries such as symmetries of 2-fold fabrics. Third, we considered decomposition of only 2.5D flat shell structures. In order to construct curved shell structures, one may need more than one unique shape for a tile. Generating GATs for curved boundaries needs to be explored in detail. Finally, and most importantly, our work currently allows only for the *forward design* of space-filling tiles. However, what would be more interesting for structural applications is to be able to specify desired physical characteristics to automatically configure the weave-symmetries and Voronoi sites to create GATs. While we initiated structural characterization in this work, we believe that a much deeper analysis of geometry-to-structure relationship needs to be developed for *inverse design* of GATs.

5.2. Generalizability

One of the main learning outcomes of our work is that Voronoi decomposition, when combined with configurations symmetries in space (e.g. weaves) and simple constructive solid geometry (CSG) operations (e.g. union) can be a powerful tool for modeling new types of geometric structures. One of the main advantages of this work that was not emphasized in prior works such as Delaunay Lofts [7] is that employing

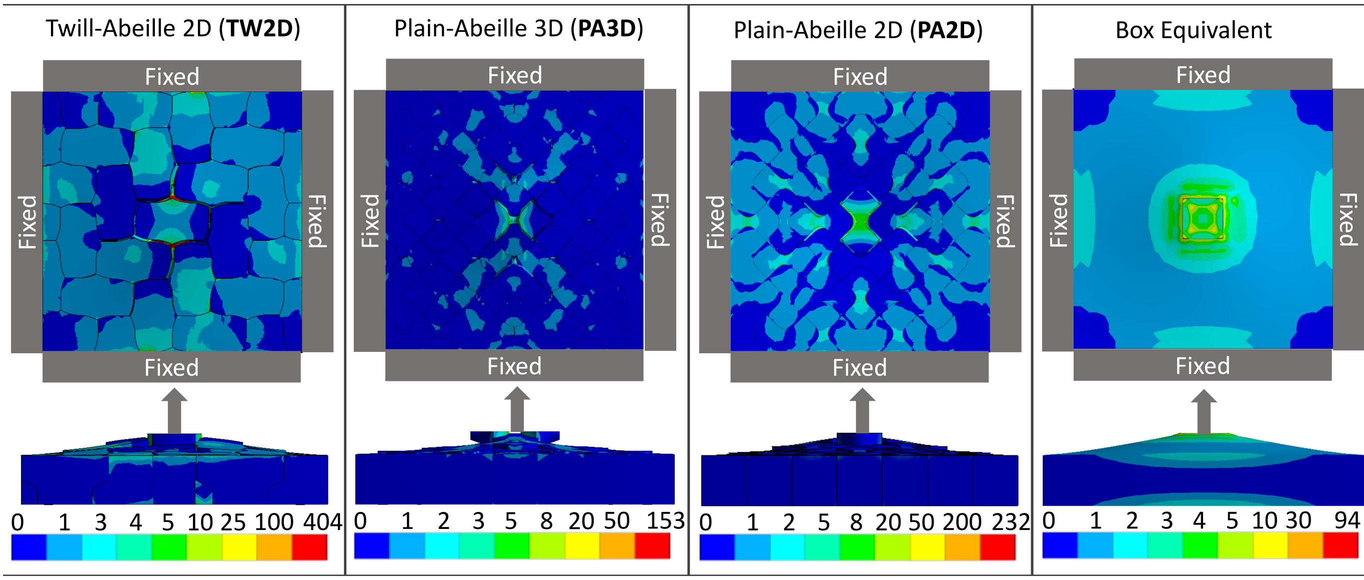

Fig. 21: (Simulation) This shows the stress distribution on a 7x7 assembly of various generated shapes. This can all be compared with the single block equivalent of these assemblies. The top and side view are shown such that the forced displacement can be seen. A displacement of 2mm was forced on the center tile. All stress values are in MPa.

higher dimensional Voronoi sites allows for generation of significantly more complex structures. This implies that while using the Voronoi makes the parts to be perfectly space filling, with further modification of control lines that define the generated shape, the assembly can potentially be made stronger and customized to a specific application. Our methodology can used by the end user to generate a variety of tilings with varying stress distribution properties allowing customized design of interlocking tiles with augmented strength of assembly.

5.3. Reciprocity

Pugnale and Sassone [43] define the principle of reciprocity to be based on "*load-bearing elements which, supporting one another along their spans and never at the extremities, compose a spatial configuration with no clear structural hierarchy*". The idea of reciprocal frames dates back to ancient Indian, Chinese, and Japanese structures in the east as well as in the works of prominent designers of the west including Leonardo's. These have recently been studied and generalized in several works [44, 43, 45] from a structural standpoint. One of the most important observations here is that reciprocal frames are essentially characterized by the topological connectivity of the constitutive load-bearing beams — a trait also present in our own framework for generating GATs. One of the main outcomes of our structural analysis is the correspondence between fabric weave symmetries and the distribution of stresses on GAT assemblies. Specifically, our analyses indicate that the mechanical properties of a given fabric woven using a specific strand pattern can provide fundamental insights regarding GAT assemblies whose shape is generated using the same weave pattern. We believe that there is an even deeper connection across weave patterns, GATs, and reciprocal frames that may lead to a systematic framework for structural analyses of such systems.

6. Conclusions & Future Directions

We presented a methodology to design space-filling tiles that we call *generalized Abeille tiles* (GATs). The key insight behind our methodology was the identification of visual correspondence between Abeille's vault shapes and bi-axial fabric weave patterns. To make this methodology operational through well-known Voronoi decomposition. To enable the exploration of the design space of GATs, we further discussed the idea of higher-dimensional (lines, surfaces etc.) sites for Voronoi decomposition. We demonstrated our methodology by designing, fabricating, and mechanically analyzing GATs as unit tiles as well as assemblies. Our structural evaluation of the unit tiles and assembled tilings revealed that there is a strong underlying relationship between the type of weave pattern, the choice of Voronoi site configuration (e.g. T-shaped, Y-shaped, etc.), and the mechanical behavior of the assemble GATs. Furthermore, our results suggest that interlocking these tiles have potential to replace existing extrusion based building blocks (such as bricks) which do not provide interlocking capability.

There are several open questions that this research poses. First, our current investigation of structural characteristics of GATs was rudimentary. It indicates a need for a more systematic approach for structural analysis. Such an approach would allow the inverse design of GATs based on desired structural properties. Second, we want to point out that woven fabrics only provide a starting point for this work. Our immediate future goal is to first extended our exploration to more general types of fabrics followed by non-fabric symmetries. The idea of exploring different spatial configurations of higher-dimensional Voronoi sites is a very fertile area for future research.

7. Acknowledgments

We thank the reviewers for their valuable feedback and comments. This work was supported by the Texas A&M Engineering Experiment Station and the J. Mike Walker '66 Department of Mechanical Engineering at Texas A&M University.

References

[1] Loeb, AL. Space-filling polyhedra. In: Space Structures. Springer; 1991, p. 127–132.

[2] Whiting, E, Ochsendorf, J, Durand, F. Procedural modeling of structurally-sound masonry buildings. ACM Trans Graph 2009;28(5):112:1–112:9. doi:10.1145/1618452.1618458.

[3] Deuss, M, Panozzo, D, Whiting, E, Liu, Y, Block, P, Sorkine-Hornung, O, et al. Assembling self-supporting structures. ACM Trans Graph 2014;33(6):214:1–214:10. doi:10.1145/2661229.2661266.

[4] Whiting, E, Shin, H, Wang, R, Ochsendorf, J, Durand, F. Structural optimization of 3d masonry buildings. ACM Trans Graph 2012;31(6):159:1–159:11. doi:10.1145/2366145.2366178.

[5] Shin, HV, Porst, CF, Vouga, E, Ochsendorf, J, Durand, F. Reconciling elastic and equilibrium methods for static analysis. ACM Trans Graph 2016;35(2):13:1–13:16. doi:10.1145/2835173.

[6] Kilian, M, Pellis, D, Wallner, J, Pottmann, H. Material-minimizing forms and structures. ACM Trans Graphics 2017;36(6):article 173. doi:http://dx.doi.org/10.1145/3130800.3130827; proc. SIGGRAPH Asia.

[7] Subramanian, SG, Eng, M, Krishnamurthy, VR, Akleman, E. Delaunay lofts: A biologically inspired approach for modeling space filling modular structures. Computers & Graphics 2019;.

[8] Estrin, Y, Dyskin, AV, Pasternak, E. Topological interlocking as a material design concept. Materials Science and Engineering: C 2011;31(6):1189–1194.

[9] Dyskin, A, Estrin, Y, Kanel-Belov, A, Pasternak, E. A new concept in design of materials and structures: Assemblies of interlocked tetrahedron-shaped elements. Scripta Materialia 2001;44(12):2689–2694.

[10] Dyskin, AV, Estrin, Y, Kanel-Belov, AJ, Pasternak, E. Topological interlocking of platonic solids: A way to new materials and structures. Philosophical magazine letters 2003;83(3):197–203.

[11] Dyskin, A, Estrin, Y, Pasternak, E. Topological interlocking materials. In: Architectured Materials in Nature and Engineering. Springer; 2019, p. 23–49.

[12] Gallon, JG. Machines et inventions approuvées par l'Academie Royale des Sciences depuis son établissement jusqu'à présent; avec leur description; vol. 7. chez Gabriel Martin, Jean-Baptiste Coignard, fils, Hippolyte-Louis Guerin ...; 1777.

[13] Borhani, A, Kalantar, N. 'apart but together: The interplay of geometric relationships in aggregated interlocking systems'. In: ShoCK!-Sharing Computational Knowledge!: Proceedings of the 35th eCAADe Conference; vol. 1. 2017, p. 639–648.

[14] Vella, IM, Kotnik, T. Stereotomy, an early example of a material system. Sharing of Computable Knowledge! 2017;:251–259.

[15] Yeomans, D. The serlio floor and its derivations. arq: Architectural Research Quarterly 1997;2(3):74–83.

[16] Pugnale, A, Parigi, D, Kirkegaard, PH, Sassone, MS. The principle of structural reciprocity: history, properties and design issues. In: The 35th Annual Symposium of the IABSE 2011, the 52nd Annual Symposium of the IASS 2011 and incorporating the 6th International Conference on Space Structures. 2011, p. 414–421.

[17] Brocato, M, Mondardini, L. A new type of stone dome based on abeille's bond. International Journal of Solids and Structures 2012;49(13):1786–1801.

[18] Weizmann, M, Amir, O, Grobman, YJ. Topological interlocking in buildings: A case for the design and construction of floors. Automation in Construction 2016;72:18–25.

[19] Evans, R. The projective cast: architecture and its three geometries. MIT press; 1995.

[20] Baverel, O, Nooshin, H, Kuroiwa, Y, Parke, G. Nexorades. International Journal of Space Structures 2000;15(2):155–159.

[21] Brocato, M, Mondardini, L. Parametric analysis of structures from flat vaults to reciprocal grids. International Journal of Solids and Structures 2015;54:50–65.

[22] Frézier, AF. La theorie et la pratique de la coupe des pierres et des bois, pour la construction des voutes et autres parties des bâtimens civils & militaires, ou Traité de stereotomie a l'usage de l'architecture; vol. 2. Doulsseker; 1738.

[23] Frézier, A. 1737 (ed. 1980): La théorie et la pratique de la coupe des pierres et des bois pour la construction des voûtes et autres parties des bâtiments civils et militaires. Nogent-le-Roy: Jacques Laget LAME 1737;.

[24] Fallacara, G. Toward a stereotomic design: Experimental constructions and didactic experiences. In: Proceedings of the Third International Congress on Construction History. 2009, p. 553.

[25] Miadragovič Vella, I, Kotnik, T, Herneoja, A, Österlund, T, Markkanen, P, et al. Geometric versatility of abeille vault. eCAADe 2016 2016;.

[26] Brocato, M, Deleporte, W, Mondardini, L, Tanguy, JE. A proposal for a new type of prefabricated stone wall. International Journal of Space Structures 2014;29(2):97–112.

[27] Brocato, M, Mondardini, L. Geometric methods and computational mechanics for the design of stone domes based on abeille's bond. Advances in Architectural Geometry 2010 2010;:149–162.

[28] Dìaz, ER. La bóveda plana de abeille en lugo. In: Actas del Segundo Congreso Nacional de Historia de la Construcción, A Coruna. 1998, p. 22–24.

[29] Fallacara, G. Digital stereotomy and topological transformations: reasoning about shape building. In: Proceedings of the second international congress on construction history; vol. 1. 2006, p. 1075–1092.

[30] Delaunay, BN, Sandakova, NN. Theory of stereohedra. Trudy Matematicheskogo Instituta imeni VA Steklova 1961;64:28–51.

[31] Schmitt, MW. On space groups and dirichlet–voronoi stereohedra. Ph.D. thesis; Berlin: Freien Universität Berlin; 2016.

[32] Grunbaum, B, Shephard, G. Satins and twills: an introduction to the geometry of fabrics. Mathematics Magazine 1980;53:139–161.

[33] Grunbaum, B, Shephard, G. Isonemal fabrics. American Mathematical Monthly 1988;95:5–30.

[34] Chen, YL, Akleman, E, Chen, J, Xing, Q. Designing biaxial textile weaving patterns. Hyperseeing: Special Issue on ISAMA'2010 2010;6(2).

[35] Ramamurthy, R, Farouki, RT. Voronoi diagram and medial axis algorithm for planar domains with curved boundaries i. theoretical foundations. Journal of Computational and Applied Mathematics 1999;102(1):119–141.

[36] Boissonnat, JD, Teillaud, M. Effective computational geometry for curves and surfaces. Berlin, Heidelberg: Springer; 2006.

[37] Gómez-Gálvez, P, Vicente-Munuera, P, Tagua, A, Forja, C, Castro, AM, Letrán, M, et al. Scutoids are a geometrical solution to three-dimensional packing of epithelia. Nature communications 2018;9(1):2960.

[38] Mughal, A, Cox, S, Weaire, D, Burke, S, Hutzler, S. Demonstration and interpretation of" scutoid" cells in a quasi-2d soap froth. arXiv preprint arXiv:180908421 2018;.

[39] Peterson, R, Terr, D, Weisstein, EW. Fundamental domain. From MathWorld–A Wolfram Web Resource. https://mathworld.wolfram.com/FundamentalDomain.html; 2020. Accessed: 2020-04-20.

[40] Khandelwal, S, Siegmund, T, Cipra, R, Bolton, J. Transverse loading of cellular topologically interlocked materials. International Journal of Solids and Structures 2012;49(18):2394–2403.

[41] Mises, Rv. Mechanics of solid bodies in the plastically-deformable state. Göttin Nachr Math Phys 1913;1:582–592.

[42] Akleman, E, Chen, J, Xing, Q, Gross, J. Cyclic plain-weaving with extended graph rotation systems. ACM Transactions on Graphics; Proceedings of SIGGRAPH'2009 2009;:78.1–78.8.

[43] Pugnale, A, Sassone, M. Structural reciprocity: critical overview and promising research/design issues. Nexus Network Journal 2014;16(1):9–35.

[44] Song, P, Fu, CW, Goswami, P, Zheng, J, Mitra, NJ, Cohen-Or, D. Reciprocal frame structures made easy. ACM Transactions on Graphics (TOG) 2013;32(4):1–13.

[45] Siegmund, T, Barthelat, F, Cipra, R, Habtour, E, Riddick, J. Manufacture and mechanics of topologically interlocked material assemblies. Applied Mechanics Reviews 2016;68(4).